ARTICLE

# Mechanical Unfolding of Ensemble Biomolecular Structures by Shear Force

Received 00th April 20xx,
Accepted 00th April 20xx

DOI: 10.1039/x0xx00000x

Changpeng Hu[+], Sagun Jonchhe[+], Pravin Pokhrel, Deepak Karna, Hanbin Mao*

Mechanical unfolding of biomolecular structures has been exclusively performed at the single-molecule level by single-molecule force spectroscopy (SMFS) techniques. Here we transformed sophisticated mechanical investigations on individual molecules into a simple platform suitable for molecular ensembles. By using shear flows inside a homogenizer tip, DNA secondary structures such as i-motifs are unfolded by shear force up to 50 pN at the 77796/s shear rate. We found that the larger the molecules, the higher the exerted shear forces. This shear force approach revealed affinity between ligands and i-motif structures. It also demonstrated a mechano-click reaction in which a Cu(I) catalyzed azide-alkyne cycloaddition was modulated by shear force. We anticipate this ensemble force spectroscopy method can investigate intra- and inter-molecular interactions with the throughput, accuracy, and robustness unparalleled to SMFS methods.

## Introduction

Mechanical properties of individual molecular structures have been probed using instruments such as optical tweezers, magnetic tweezers, and AFM.[1-4] There is no approach currently available to investigate mechanical properties of more than a few hundreds of molecular structures. The limited number is set by the field of view in magnetic tweezers[2, 4] or fluorescence microscope in which FRET (fluorescence resonance energy transfer) signals have been used to report the force for the molecules anchored in DNA origami frameworks.[5] The difficulty in measuring mechanical properties of a larger set of molecules lies in the directionality of the force. Before any mechanical manipulation can be made, different molecules must be oriented along the same direction. For single-molecule studies, such a requirement is trivial as only one molecule needs to be aligned. However, for millions of molecules at the ensemble level, it is insurmountable by current instruments to align these molecules before probing their mechanical properties.

Shear flow offers a potential solution to orient a large set of molecules. In a liquid stream, the no-slip condition dictates that the speed of the fluid at the boundary is zero, while that at middle of the flow is fastest.[6] Such a gradient in flow speed incurs a shear stress applied parallel to the surface of the boundary. When the shear force is higher than the entropic recoiling force of a polymer for example, the polymer gets stretched by the tensile force applied along their long axes (Figure 1A). As long as the flow direction and the variation in the flow rate are maintained, all identical molecules in such a flow stream will take the same orientation along which the same force can be applied.

In this work, we used the shear flow generated in a homogenizer tip to mechanically unfold biomolecules as exemplified by human telomeric DNA i-motif structures.[7] Using a pair of FRET dyes, we monitored the behavior of the i-motif at a shear rate of 9724-97245 /s. These shear rates are equivalent to 17-50 pN mechanical force after comparison with mechanical unfolding of the same DNA structure in optical tweezers. In the presence of an i-motif ligand, L2H2-4OTD[8], less unfolding was observed for i-motif under the same shear force, consistent with increased mechanical stability of the L2H2-4OTD bound i-motif. Such a strategy allowed us to reveal a dissociation constant of 36 mM for the L2H2-4OTD binding to the i-motif, a value consistent with that obtained by single-molecule mechanical unfolding in optical tweezers (31 mM) and close to that measured by gel shift.[8] Next, we used the shear force to unfold i-motifs, which exposed chelated Cu(I) ions to catalyze a fluorogenic click reaction.[9] Using this so-called mechano-click chemistry, we were able to reveal the relationship between the shear force and the size of the i-motif modified with flanking ssDNA fragments. We found that the longer the flanking sequence of the i-motif, the higher the shear force, and the faster the click reaction. Given that the shear force approach drastically increased the throughput of the force spectroscopy to an unprecedented level, we anticipate this new method will accurately elucidate mechanobiological and mechanochemical processes at the unprecedented ensemble level.

## Results and discussion

### Unfolding of i-motif in shear flow.

To demonstrate that the shear stress is able to mechanically unfold an ensemble set of biomolecular structures, we generated a rotational shear flow in a homogenizer generator (see SI), which contains a rotor (Figure 1A, external diameter,

[a.] *Department of Chemistry & Biochemistry and School of Biomedical Sciences, Advanced Materials and Liquid Crystal Institute, Kent State University Kent, OH 44242 (USA) E-mail: hmao@kent.edu*

[b.] [+] *These authors contributed equally to this work.*

Electronic Supplementary Information (ESI) available: [details of any supplementary information available should be included here]. See DOI: 10.1039/x0xx00000x

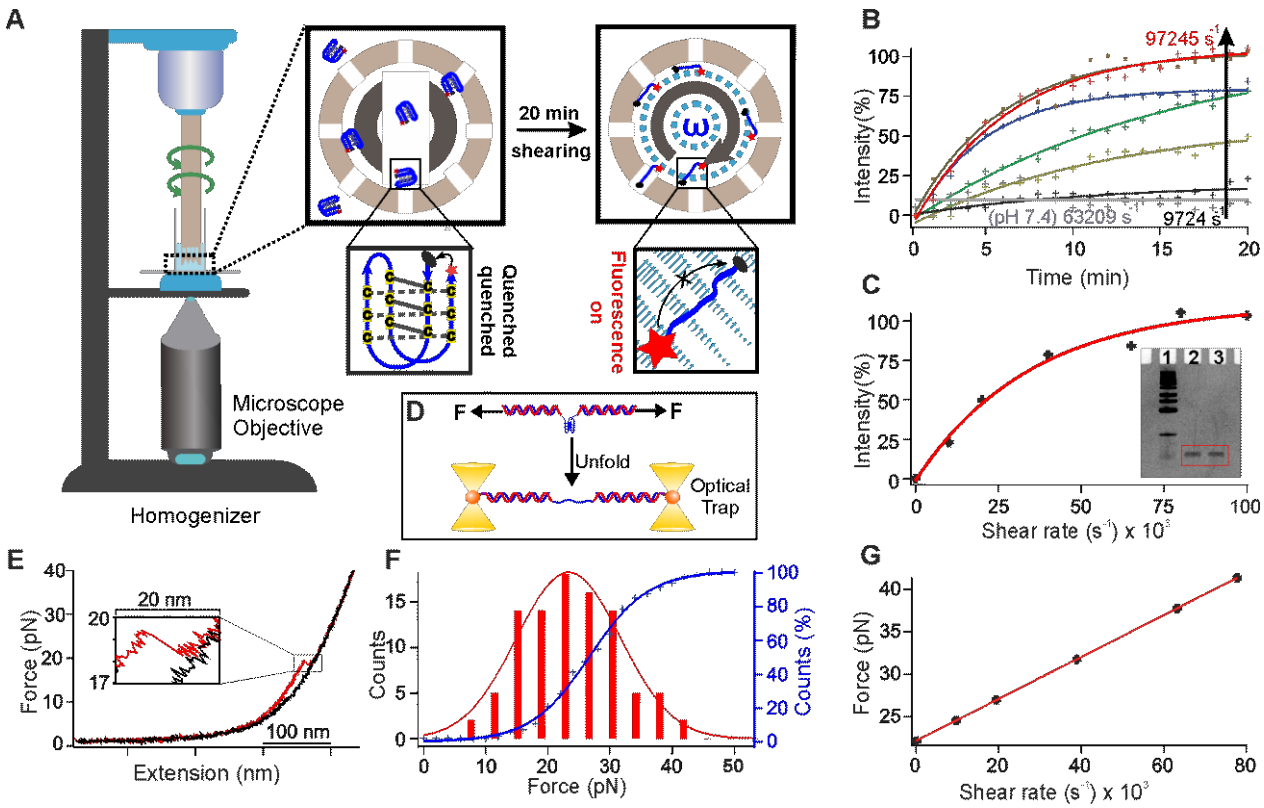


**Figure 1.** Unfolding of i-motif in shear flow. A) Schematic of unfolding of a FRET pair (Cy5 and qFlamma® Black01) labelled i-motif (Oligo 5, Table S1) by the shear flow generated in a benchtop homogenizer. B) Real time increase of fluorescence intensity due to unfolded the i-motif at different shear rates. C) Shear rate vs percentage of increased fluorescence intensity after 20 min shearing. Inset shows the image of 15% denatured PAGE for the 27 nt i-motif at the 63209/s shear rate for 20 min (lane 1, marker; lane 2, before shearing; lane 3, after shearing). D) Schematic of the single-molecule mechanical unfolding of the human telomeric i-motif (Oligo 3, Table S1) in optical tweezers. E) A typical force-extension curve of unfolding the i-motif at pH 5.5 supplemented with 100 mM KCl. F) Unfolding force histogram for the i-motif (left axis) and cumulative unfolding percentage vs force (right axis) histogram. G) Diagram of the shear rate vs shear force for the i-motif sequence shown in (A). Red line depicts a linear fitting.

5.00 mm) and a stator (internal diameter, 5.11 mm). While the stator remains still, the speed of the rotor can be adjusted to generate a rotational velocity up to 20000 rpm, which is equivalent to a shear rate of 92745 /s for this homogenizer. We anticipated biomolecular structures may be mechanically unfolded under such a high shear rate. We used DNA i-motif formed in the human telomeric sequence, 5'-TAA$(CCCTAA)_4$,[7, 10] as an exemplary biomolecular structure to test our hypothesis. By attaching a FRET pair of fluorescence molecules, Cy5 and qFlamma® Black01, to the 5' and 3' ends of the telomeric sequence respectively (Oligo 5, Table S1), the folded i-motif will not show fluorescence since Cy5 is quenched by the qFlamma® Black01 due to close distance of the two dyes. Upon unfolding of the i-motif, the distance between the Cy5 and qFlamma® Black01 is too long to carry out efficient energy transfer, causing the recovery of the Cy5 fluorescence (Figure 1A).

To observe fluorescence signals, the homogenizer was placed on top of an inverted fluorescence microscope (Figure 1A, see SI). We then dissolved 5 μM FRET-pair labelled C-rich telomeric sequence (Oligo 5, Table S1) in 300 μL 10 mM MES buffer supplemented with 100 mM KCl at pH 5.5. It has been well known that i-motif was folded at pH 5.5 [7], which was confirmed by circular dichroism (CD) data (Figure S1). Folded i-motif generated ~1 nm end-to-end distance[10] between the Cy5 and qFlamma® Black01, a value facilitating the Cy5 quenching by the qFlamma® Black01. Indeed, before the rotor was turned on, we observed low Cy5 fluorescence intensity. When the shear flow was established with a shear rate ranging from 9724 to 97245 /s in the homogenizer, we observed a gradual increase in the fluorescence intensity (Figure 1B). Turning off the shear flow reversed the trend of the signal change (Figure S2). All these observations suggested that the shear flow was able to mechanically unfold DNA i-motif structures. As a control, we repeated experiments for the same i-motif in the MES buffer at pH 7.4, we found fluorescence increase was not observed under the shear rate of 63209 /s (Figure 1B). Since i-motif does not form at pH 7.4, this result confirmed that the fluorescence increase is due to the unfolding of the i-motif in the shear flow. The rate in the fluorescence signal increase was dependent on the shear rate (Figure 1B&C), which was consistent with the fact that the higher the shear rate, the more the shear force, and the faster the unfolding rate of the i-motif. To rule out the fluorescence increase is not due to the break of the i-motif forming DNA under shearing, we examined the integrity of the DNA strands after shear flows. We found negligible breakdown of the DNA strands at the shear rate of 63209 /s (Figure 1C inset, lane 2: before shearing; lane 3: after shearing).

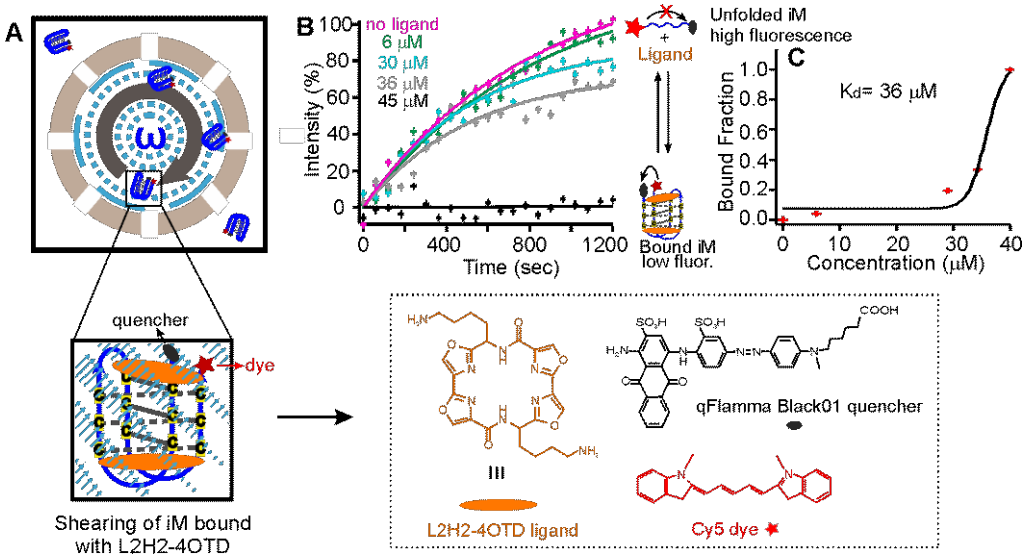


**Figure 2.** Unfolding of ligand-bound telomeric i-motif. A) Schematic of shearing a FRET-pair (Cy5 and qFlamma® Black01) labelled telomeric i-motif (Figure 1A) bound with the L2H2-4OTD ligand. B) Percentage fluorescence intensity of the i-motif versus shearing time at different concentrations of ligand (0, 6, 30, 36, and 45 μM). C) Binding curve of the i-motif at different concentrations of L2H2-4OTD. Black curve represents the Hill's fitting (see SI).

At ~20 min of shearing, the fluorescence intensity reached a plateau (Figure 1B) under different shear rates, indicating a steady state was reached. When we plotted the plateau fluorescence intensity vs shear rate, we observed that the fluorescence intensity did not change any more at the shear rate above 97245 /s (Figure 1C), suggesting that the associated shear force was already higher than that required to unfold the i-motif. We therefore used the fluorescence intensity at 20 mins at the 97245 /s shear rate as a reference point to calculate the percentage of unfolded i-motif structures at any time for different shear rates.

To calibrate the mechanical force under specific shear rate, we compared the percentage unfolding of the i-motif with that obtained by mechanical unfolding of the same i-motif structure in optical tweezers in the same buffer and pH[11] (Figure 1D, see SI for details). In force-extension (F-X) curves of the i-motif (see a typical curve in Figure 1E and more curves in Figure S3), we observed a rupture event (blowup in Figure 1E) from which unfolding force and accompanied change in contour length ($\Delta L$) can be retrieved. The $\Delta L$ value (7.6 nm) is consistent with that of the telomeric i-motif (Figure S4, expected $\Delta L$: 8.0 nm; see SI for $\Delta L$ calculations), confirming the rupture event was indeed due to the unfolding of the i-motif. After integration of the unfolding force histogram for this i-motif (Figure 1F), we obtained the cumulative unfolding percentage at a particular mechanical force (blue curve in Figure 1F). Assuming that percentage unfolding of the i-motif is equivalent between single molecule mechanical unfolding experiment (Figure 1E) and shear force experiment (Figure 1C) at a particular force, we calibrated the shear force vs shear rate in Figure 1G, which depicted that up to 41 pN can be applied to the FRET-pair labelled i-motif at the shear rate of 77796 /s. Given that the shear force is dependent on the size of the object inside the shear flow[6], even higher force can be generated if elongated handles such as DNA strands can be attached to molecular structures (see below). We anticipate such a shear flow method can transform single-molecule force spectroscopy, which is amenable to only a few molecules, into an ensemble force spectroscopy suitable for a large set of molecules in solution.

**Evaluation of ligand binding to biomacromolecules in shear flow.**

To demonstrate the capability of this new ensemble force spectroscopy approach, we used the shear flow to evaluate the binding complex between i-motif and L2H2-4OTD.[8] L2H2-4OTD is a compound that can bind to i-motif structures with a dissociation constant (*K*d) in micromolar range.[8] After the above-mentioned Cy5 and qFlamma® Black01 labelled i-motif (Oligo 5, Table S1) was mixed with the L2H2-4OTD at different concentrations (6-45 mM) in the same buffer, the mixture was subjected to the shear force generated in the homogenizer (Figure 2). We anticipated more Cy5 fluorescence would be quenched by qFlamma® Black01 at a particular shear rate since the unfolding of the i-motif became more difficult upon the ligand binding[12]. Indeed, when we evaluated the unfolding force of the L2H2-4OTD bound i-motif (Figure S5), we found an average unfolding force of ~33 pN (Figure S6). Based on this force, we chose 63209 /s as the shear rate, which was expected to produce 38 pN on the 27 nt i-motif (Figure 1G). Such a force was sufficient to unfold free i-motif (23 pN) but would not unfold all L2H2-4OTD bound i-motif.

We found that increment in the fluorescence intensity became less obvious with increasing L2H2-4OTD concentrations (Figure 2B), which was expected as more i-motifs were bound with the ligands when concentration of the L2H2-4OTD increased. After using single exponential fitting to these temporal traces, we retrieved the plateau values as the steady-state signals around 20 min, from which the binding percentage of i-motif was calculated by interpolation against the curve without ligand (0% binding) and that with 45 mM ligand (100% binding). These binding fractions were then plotted against the free ligand concentration (Figure 2C). Using Hills equation[13] (see SI), we retrieved a *K*d of 31 mM between the L2H2-4OTD and i-motif. Single-molecule mechanical unfolding of the same i-motif in presence of the L2H2-4OTD generated a similar *K*d (31 mM) in optical tweezers (Figure S7). This *K*d is also comparable to that measured by gel shift (105 μM)[8]. These results

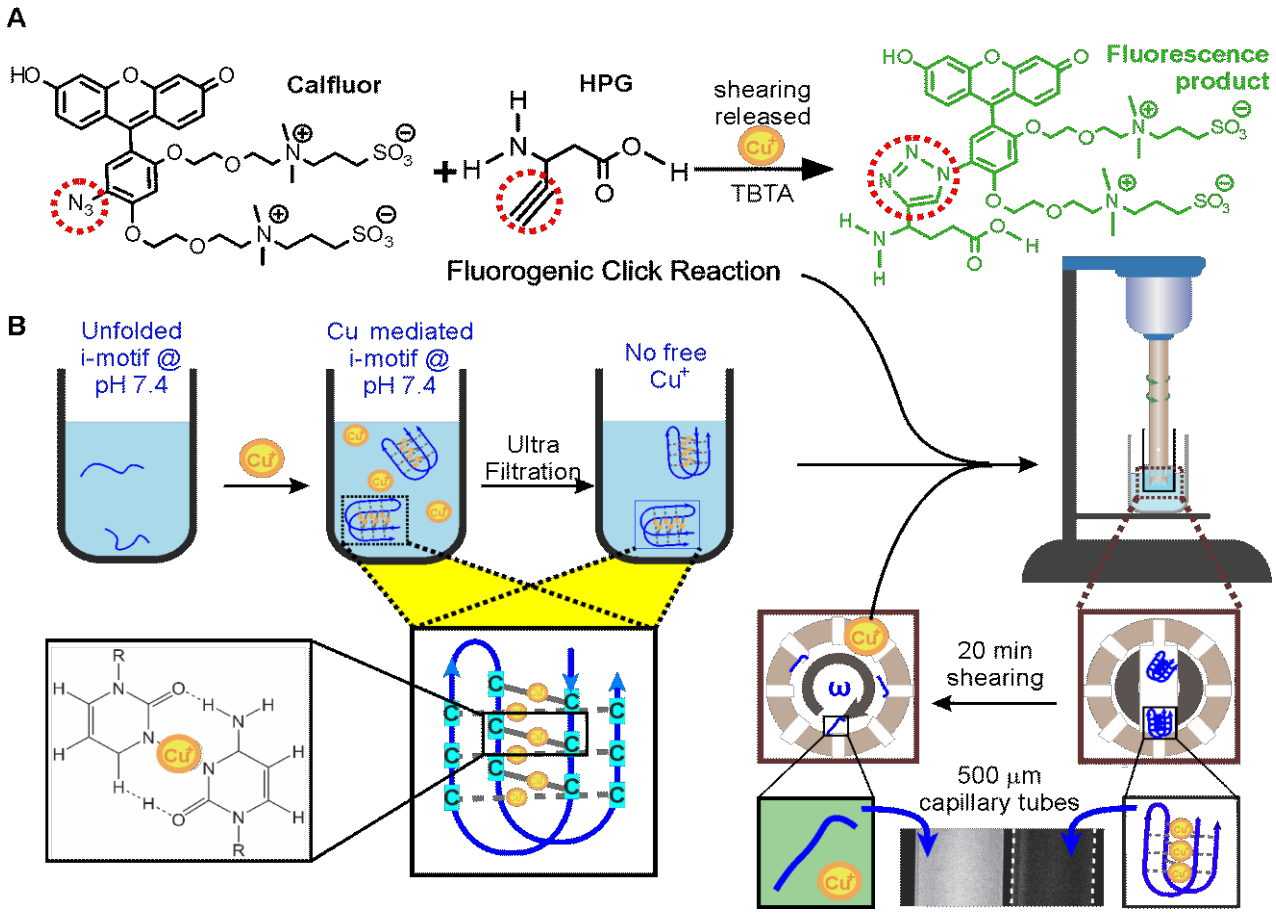


**Figure 3.** Mechano-click reactions. A) A fluorogenic click reaction between Calfluor® and HPG (L-Homopropargylglycine). The product of the click reaction emits green light. B) The telomeric i-motif chelated with Cu+ at pH 7.4 was filtered to remove excess Cu+ in solution. The Cu+ chelated i-motif was unfolded by shear flow in the homogenizer. The released Cu+ catalyzed the fluorogenic Calfluor and HPG click reaction, which was observed in capillary tubes of 500 μm width (bottom).

validated the accuracy of our shear flow based mechanical unfolding approach.

**Shear force actuated click reaction.**

Efficient and quantitative click reactions[14] have been widely used in many fields such as biosensing, drug development, and materials preparations. Here, we demonstrate a click reaction that is responsive to shear force. To evaluate the efficiency of the click reaction under the shear force, we chose a fluorogenic Cu(I)-catalyzed azide-alkyne cycloaddition (CuAAC) (Figure 3A).[15] Upon cycloaddition, the product of this reaction emits green fluorescence, which will be recorded in our instrument for shear flow experiments.

The same i-motif forming DNA, 5'- $(TAACCC)_4$ TAA (Oligo 3, Table S1), was used as a carrier for the Cu(I) catalyst. At pH 7.4, it has been found that i-motif can fold due to the chelation of the Cu(I) ions to the cytosine:cytosine pairs (Figure 3B)[9], which was confirmed by CD signatures (Figure S1). Since this i-motif can be unfolded under the shear force (Figure 1), we expected the chelated Cu(I) would be exposed to the solution to catalyze the fluorogenic CuAAC reaction. To test this hypothesis, we first mixed 10 μM i-motif forming sequence with 150 μM Cu(I) in 30 mM Tris buffer at pH 7.4 for 10 minutes. We supplied 300 μM ascorbic acid in each experiment to prevent the oxidation of the Cu(I). Amicon® filter (MWCO 3K) was then used to filtrate out any free Cu(I) to reduce the background click reaction catalyzed by these Cu(I) ions. A shear rate of 63209 /s was finally applied to the reaction mixture that contained two click reactants and TBTA[16] (Figure 3). This shear rate was chosen to ensure that the i-motif (mechanical stability ~23 pN in Figure 1F) can be readily unfolded mechanically by the shear flow (see Figure 1G, 38 pN). As expected, we observed increased fluorescence after shearing, indicating that Cu(I) was indeed available for click reaction due to the unfolding of i-motif by shear force (Figures 3B&4A). As a control, the filtered Cu(I)-chelated i-motif at pH 7.4 was subjected to random mechanical perturbation by 20 min vortexing. Only a little florescence increase was observed (Figure 4B), indicating it was the stretching shear force, not the random vortexing force, that unfolded the i-motif. In other controls, little fluorescence increase was observed for a telomeric G-quadruplex forming DNA (4G) [17, 18], 5'- $(TTAGGG)_4$ TTA, or a structureless scrambled sequence (s4G), 5'-TGA GTG TGA GTG TGA GTG TGA GTG TAT, (Figure 4B), which firmly supported that it was the Cu(I) chelated i-motif that catalyzed the fluorogenic CuAAC reaction under the shear force. We anticipate this mechano-click reaction can provide a unique modulation with little background for click chemistry. Since

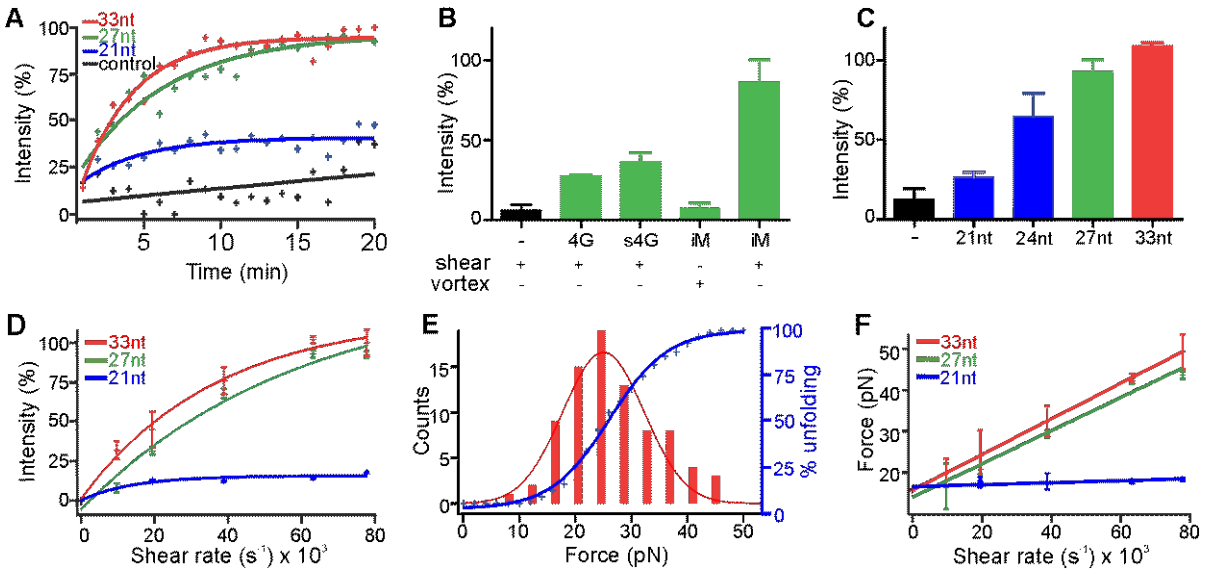


**Figure 4.** Shear force is determined by the molecular size in the shear flow. A) Fluorescence intensity of the click reaction shown in Figure 3 increased over time at the 63209/s shear rate. The 33nt, 27nt, and 21nt depict i-motif forming sequences with different lengths of flanking DNA (see text for details). Control represents no DNA. B) Shear force, not the vortex force, triggered the fluorescent click reaction. The fluorescence intensities were taken at the 20 min of respective actions. The 4G, s4G, and iM depict G-quadruplex forming sequence (Oligo 13, Table S1), scrambled sequence (Oligo 14), and the 27nt i-motif forming sequence (Oligo 3), respectively. The black bar depicts a sample without DNA. C) Length of the telomeric i-motif sequence vs the fluorescence intensity of the click product at 20 min shearing of 63209/s shear rate. D) Shear rate vs percentage of increased fluorescence intensity for i-motif fragments with different length. E) Unfolding force histogram (left) and cumulative unfolding percentage (right axis) of the 27nt i-motif sequence in presence of 150 μM Cu+ in 30 mM Tris buffer supplemented with 300 mM ascorbic acid and 100 mM KCl at pH 7.4. (F) Diagram of shear rate vs shear force for the telomeric i-motif sequence with different length. All the lines depict linear fittings.

FRET pairs are no longer needed in the construct preparation, it also provides an affordable approach to investigate the mechanical effect on biomolecular structures.

This affordable mechano-click reaction was subsequently used to elucidate the molecular size effect on the shear force (Figure 4 A, C, D, and F). To vary the molecular size, we changed the length of the flanking sequence linked to the i-motif core (underlined), 5'- $(TAA)_m(CCCTTA)_3CCC(TAA)_n$, where m = n = 0, 1, and 2 stand for the 21nt, 27nt, and 33nt oligos, respectively; for the 24nt DNA, m=1 and n=0. These DNA sequences were complexed with Cu(I), filtered with the Amicon® membrane (see above), and subjected to the shear flow at the 63209 /s shear rate. The fluorogenic CuAAC reactions showed increased fluorescence intensity over time for all these i-motif constructs (Figure 4A). Significantly, we found that the catalytic efficiency was increased with the length of the flanking sequence (Figure 4 A&C). This observation directly supported that the longer the flanking sequence, the higher the shear force experienced by the DNA construct. As expected, we also found that efficiency of the CuAAC reactions increased with the shear rate (Figure 4D). Finally, assuming all i-motif was unfolded at the 63209 /s shear rate for either the 27 nt or 33 nt i-motif construct, we estimated the percentage unfolding of the i-motif from the CuAAC click reaction and compared with that obtained from single-molecule unfolding in optical tweezers (Figure 4E, i-motif chelated with Cu(I) in a pH 7.4 buffer, see Figures S8&S9 for F-X curves and $\Delta L$ histogram, respectively). The resultant shear force vs shear rate calibration (Figure 4F) confirmed the effect of the molecular size on the shear force: the longer the molecule, the higher the shear force.

## Conclusions

In summary, we have successfully invented a shear flow based mechanical unfolding approach to investigate mechanical properties of an ensemble set of molecular structures. With this ensemble force spectroscopy method, we found up to 50 pN force was generated on DNA i-motif structures. We demonstrated a new type of click reaction that can be actuated by shear forces. We confirmed that the shear force experienced by molecules increased with molecular size. This gave future direction to generate even higher force after molecules are attached with elongated handles such as polymers or nanoparticles.

## Conflicts of interest

There are no conflicts to declare.

## Acknowledgements

This research work was supported by National Science Foundation [CBET-1904921] and National Institutes of Health [NIH R01CA236350] to H.M.

## Notes and references


1. M. T. Woodside, W. M. Behnke-Parks, K. Larizadeh, K. Travers, D. Herschlag and S. M. Block, *Proc. Natl. Acad. Sci. U S A*, 2006, **103**, 6190-6195.
2. I. Vilfan, J. Lipfert, D. Koster, S. Lemay and N. Dekker, in *Handbook of Single-Molecule Biophysics*, eds. P. Hinterdorfer and A. Oijen, Springer US, 2009, ch. 13, pp. 371-395.
3. M. Grandbois, M. Beyer, M. Rief, H. Clausen-Schaumann and H. E. Gaub, *Science*, 1999, **283**, 1727-1730.
4. T. Strick, J.-F. Allemand, D. Bensimon and V. Croquette, *Biophys. J.*, 1998, **74**, 2016-2028.
5. P. C. Nickels, B. Wünsch, P. Holzmeister, W. Bae, L. M. Kneer, D. Grohmann, P. Tinnefeld and T. Liedl, *Science*, 2016, **354**, 305.
6. I. B. Bekard, P. Asimakis, J. Bertolini and D. E. Dunstan, *Biopolymers*, 2011, **95**, 733-745.
7. K. Gehring, J. L. Leroy and M. Guéron, *Nature*, 1993, **363**, 561-564.
8. S. Sedghi Masoud, Y. Yamaoki, Y. Ma, A. Marchand, F. R. Winnerdy, V. Gabelica, A. T. Phan, M. Katahira and K. Nagasawa, *ChemBioChem*, 2018, **19**, 2268-2272.
9. M. A. Abdelhamid, L. Fábián, C. J. MacDonald, M. R. Cheesman, A. J. Gates and Z. A. Waller, *Nucleic Acids Research*, 2018, **46**, 5886-5893.
10. S. Dhakal, J. D. Schonhoft, D. Koirala, Z. Yu, S. Basu and H. Mao, *J. Am. Chem. Soc.*, 2010, **132**, 8991–8997.
11. Y. Cui, D. Kong, C. Ghimire, C. Xu and H. Mao, *Biochemistry*, 2016, **55**, 2291-2299.
12. D. Koirala, S. Dhakal, B. Ashbridge, Y. Sannohe, R. Rodriguez, H. Sugiyama, S. Balasubramanian and H. Mao, *Nat. Chem.*, 2011, **3**, 782-787.
13. D. Voet and J. G. Voet, *Biochemistry*, John Wiley and Sons, Inc., New York, 2nd edn., 1995.
14. H. C. Kolb, M. G. Finn and K. B. Sharpless, *Angew. Chem. Int. Ed. Engl.*, 2001, **40**, 2004- 2021.
15. P. Shieh, V. T. Dien, B. J. Beahm, J. M. Castellano, T. Wyss-Coray and C. R. Bertozzi, *Journal of the American Chemical Society*, 2015, **137**, 7145-7151.
16. T. R. Chan, R. Hilgraf, K. B. Sharpless and V. V. Fokin, *Organic Letters*, 2004, **6**, 2853-2855.
17. Z. Yu, J. D. Schonhoft, S. Dhakal, R. Bajracharya, R. Hegde, S. Basu and H. Mao, *J. Am. Chem. Soc.*, 2009, **131**, 1876-1882.
18. F. F. W. J. Smith, *Nature*, 1992, **356**, 164-168.